(40) (a) C. Walling and A. Padwa, *J. Am. Chem. Soc.*, **85**, 1593 (1963); (b) *ibid.*, **85**, 1587 (1963).
(41) C. Walling and J. A. McGuiness, *J. Am. Chem. Soc.*, **91**, 2053 (1969).
(42) (a) C. Walling and B. B. Jacknow, *J. Am. Chem. Soc.*, **82**, 6108, 6113 (1960); (b) C. Walling and W. Thalen, *ibid.*, **83**, 3877 (1961).
(43) K. U. Ingold in "Free Radicals", J. K. Kochi, Ed., Vol. I, Wiley, New York, N.Y., 1973, Chapter 2.
(44) J. K. Kochi, ref 43, Chapter 23.
(45) We gratefully acknowledge the assistance of Mr. John B. Raff, who determined the rate constants for the substituted *tert*-butyl perbenzoates.
(46) J. Shorter, "Correlation Analysis in Organic Chemistry", Clarendon Press, Oxford, 1972.
(47) Similar small effects have been observed in the acid-catalyzed esterification of benzoic acids ($\rho = -0.52$)[46] and in the thermolysis of *tert*-butyl peresters ($\rho = -0.56$).[46] Cleavage of the O–O bond in the latter reaction is more facile when the bond is less polar.
(48) A. T. Blomquist and I. A. Berstein, *J. Am. Chem. Soc.*, **73**, 5546 (1951).
(49) K. L. Scott and A. G. Sykes, *J. Chem. Soc., Dalton Trans.*, 1832 (1972).
(50) Unlike the inorganic situation, in the case of the perbenzoate, ^{18}O tracer experiments appear feasible in that it is possible to label each oxygen specifically, such as $t\text{-Bu}^{18}O^{16}OC(^{16}O)Ph$ and $t\text{-Bu}^{16}O^{18}OC(^{18}O)Ph$. The experiment requires a knowledge of the mode of cleavage during the subsequent acid hydrolysis of the Cr(III) carboxylate, which for $(H_2O)_5CrO_2CCH_3^{2+}$ was inferred to occur at the C–O bond (E. A. Deutsch and H. Taube, *Inorg. Chem.*, **7**, 1532 (1968)), a conclusion which would also be verified.
(51) Experimental values of k_1 for the symmetric peroxides have been divided by a statistical factor of two.
(52) S. Hasegawa, N. Nishimura, S. Mitsumoto, and K. Yokoyama, *Bull. Chem. Soc. Jpn.*, **36**, 522 (1963).
(53) Another likely source of hydroxymethyl radical is its formation from reaction of $C_6H_5\cdot$ with methanol solvent (eq 23a).[54]

$$C_6H_5\cdot + HCH_2OH \rightarrow C_6H_6 + \cdot CH_2OH \qquad (23a)$$

(54) J. E. Packer, D. B. House, and E. J. Rasburn (*J. Chem. Soc. B*, 1574 (1974)) give $k_{23a} > 1.4 \times 10^5\ M^{-1}\ s^{-1}$.
(55) R. Hiatt in "Organic Peroxides", Vol. II, D. Swern, Ed., Wiley, New York, N.Y., 1971, Chapter VIII.

The Molybdenum–Molybdenum Triple Bond. 1. Hexakis(dimethylamido)dimolybdenum and Some Homologues: Preparation, Structure, and Properties

M. H. Chisholm,*[1a] F. A. Cotton,*[1b] B. A. Frenz,[1b] W. W. Reichert,[1a] L. W. Shive,[1b] and B. R. Stults[1b]

Contribution from Departments of Chemistry, Princeton University, Princeton, New Jersey 08540, and Texas A&M University, College Station, Texas 77843. *Received November 3, 1975*

Abstract: $Mo_2(NR_2)_6$, where $NR_2 = NMe_2$, NMeEt, and NEt_2, have been prepared from metathetic reactions involving molybdenum halides and the appropriate lithium dialkylamide, and have been characterized by a number of physical techniques. The molecular structure of $Mo_2(NMe_2)_6$ has been determined by single-crystal x-ray diffraction. The space group is $P2_1/c$ with $a = 11.461$ (3) Å, $b = 12.052$ (4) Å, $c = 15.409$ (3) Å, $\beta = 101.83$ (2)°, $V = 2083.3$ (10) Å^3, and $Z = 4$. The molecules lie on centers of inversion and form two crystallographically independent pairs. The two molecules are essentially identical, each having virtual S_6 symmetry; the central Mo_2N_6 skeleton has virtual D_{3d} symmetry, i.e., ethane-like geometry. The Mo–Mo distances are 2.211 (2) and 2.217 (2) Å. The following mean distances and angles were found: Mo–N, 1.98 Å; N–C, 1.47 Å; Mo–Mo–N, 103.7°. The bonds to N are essentially coplanar. The structure has been refined to $R_1 = 0.057$ and $R_2 = 0.075$ using 1897 reflections having $I > 3\sigma(I)$. The short Mo–Mo distance together with other structural and physicochemical properties establish the presence of a Mo–Mo triple bond. The orientations of the planar $MoNC_2$ units lead to six proximal and six distal methyl groups with respect to the Mo–Mo bond. Variable temperature ^1H NMR studies show that proximal and distal methyl groups are frozen out in solution below −30°; at higher temperatures they interconvert rapidly on the NMR time scale. A large chemical shift separation, ca. 2 ppm, between proximal and distal methyl proton resonances reflects the marked diamagnetic anisotropy of the Mo–Mo triple bond. $Mo_2(NMeEt)_6$ and $Mo_2(NEt_2)_6$ show similar ^1H NMR spectra: $Mo_2(NMeEt)_6$ exists in an equilibrium of isomers favoring proximal methyl and distal ethyl groups. No single Raman active band can be assigned to a totally symmetric Mo–Mo stretching vibration due apparently to extensive coupling between this and other vibrational modes. The bonding and structural properties of $Mo_2(NR_2)_6$ are compared with previously reported alkyls, Mo_2R_6, and with related chromium(III) alkyls, dialkylamides, and alkoxides.

The element molybdenum has already been found to be a prolific former of homonuclear metal-metal bonds, especially quadruple ones.[2] A distinct capacity to form triple bonds has also become evident, somewhat more recently. The first triple bond was found[3] in $Mo_2(CH_2SiMe_3)_6$, where the bond length was found to be 2.167 Å and the second[4] in $Mo_2(NMe_2)_6$ where the bond length is 2.214 (2) Å. Most recently, the compound $[(\eta^5\text{-}C_5H_5)Mo(CO)_2]_2$ has been shown[5] to have a (presumably) triple bond with a length of 2.448 (1) Å, that is, about 0.25 Å longer than in the other two cases.[6]

In the meantime, in our laboratories several compounds containing tungsten-tungsten triple bonds have been prepared and characterized.[7] In this and the two following papers[8,9] we shall describe the preparation, structures, and certain other properties of these new molybdenum and tungsten compounds in detail. Preliminary reports on $Mo_2(NMe_2)_6$ have appeared.[4,10]

Results and Discussion

Synthesis. Analysis of the crude brown product obtained from petroleum extraction of the reaction between $MoCl_5$ and $LiNR_2$ (5 equiv) indicated[11] molybdenum to nitrogen ratios of ca. 1:3.2 and showed valencies of molybdenum somewhat greater than 3. The monomeric compounds $Mo(NR_2)_4$ were then obtained by sublimation at 60–90° ($Mo(NMe_2)_4$) and 80–110° ($Mo(NEt_2)_4$) at 10^{-4} cmHg. Analysis of the residue after sublimation gave molybdenum to nitrogen ratios of ca. 1:2.6 and suggested valencies of molybdenum less than 3. This situation was reminiscent of the behavior of many of the dialkylamides of titanium(III), vanadium(III), and chromium(III) which readily undergo disproportionation under vacuum at relatively mild temperatures,[12] e.g.,

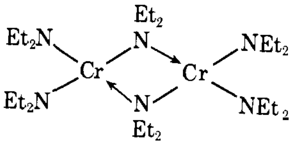

$$\longrightarrow [Cr(NEt_2)_2]_n + Cr(NEt_2)_4 \quad (1)$$

However, in contrast to these first-row transition metal tris(dialkylamides) which show only ions derived from $M(NR_2)_4{}^+$ in the mass spectrum, the crude materials of approximate composition $Mo(NR_2)_3$ showed dinuclear species such as $Mo_2(NR_2)_6{}^+$. We therefore decided to investigate further the dark brown pyrophoric residues which remained after sublimation of $Mo(NR_2)_4$.

Substantial amounts of these residues were soluble in alkane solvents. Extraction with pentane or hexane followed by stripping off the solvent led to brown solids which again yielded $Mo(NR_2)_4$ on sublimation. However, at higher temperatures (100–120° (NMe_2), 120–150° (NEt_2) at 10^{-4} cmHg) small amounts of yellow crystalline compounds also sublimed. When the process of petroleum extraction followed by sublimation was repeated the yield of the yellow crystalline solids increased relative to $Mo(NR_2)_4$.

Careful fractional sublimation allowed the isolation of the yellow solids which could then be purified by subsequent resublimation and crystallization. Analysis and subsequent characterization showed that these yellow crystalline substances were $Mo_2(NR_2)_6$.

We have therefore established that the crude product from the reaction of $MoCl_5$ and $LiNR_2$ (5 equiv) was a mixture of $Mo(NR_2)_4$, $Mo_2(NR_2)_6$, and other nonvolatile species of lower-valent molybdenum. The nature of the oxidized organic products and the lower-valent molybdenum species is not known at this time. We have, however, established that compounds of formula $Mo_2(NR_2)_6$ are stable with respect to disproportionation to give $Mo(NR_2)_4$.

Since the $Mo_2(NR_2)_6$ compounds provide excellent starting materials for the synthesis of other metalloorganic compounds of molybdenum(III) it was particularly desirable to obtain an improved synthesis. A logical starting point was to use metathetic reactions involving $MoCl_3$. However, our initial work using commercial sources of $MoCl_3$ was disappointing and gave erratic results. Significant quantities of $Mo(NR_2)_4$ were often obtained. This suggested that either the reaction conditions were very critical or that some impurities in $MoCl_3$ were responsible for the formation of $Mo(NR_2)_4$. Examination of commercially available samples of $MoCl_3$ showed that they often contained significant quantities of $MoCl_5$ and volatile oxymolybdenum chlorides. When freshly prepared $MoCl_3$, free from $MoCl_5$ and oxymolybdenum chlorides, was used we obtained reproducible results. $Mo_2(NMe_2)_6$ was obtained in ca. 20–30% yield based on the reaction between $MoCl_3$ and $LiNMe_2$ (3 equiv). Although only a trace of $Mo(NMe_2)_4$ was obtained in the preparation of $Mo_2(NMe_2)_6$, analogous reactions involving LiNMeEt and $LiNEt_2$ gave significant quantities of $Mo(NR_2)_4$, (NEt_2, NMeEt) which thus necessitated the separation procedures described previously. The difference between the reactions involving $LiNMe_2$ and $LiNEt_2$ is quite striking in this respect. Models of the dinuclear diethylamide, $Mo_2(NEt_2)_6$, suggest that it is an extremely crowded molecule. Thus, it is not unreasonable to suppose that during the reaction between $LiNEt_2$ and molybdenum(III) chloride the formation of $Mo(NEt_2)_4$ by a redox reaction competes with the formation of the sterically crowded $Mo_2(NEt_2)_6$. Attempts to synthesize $Mo_2(NR_2)_6$ using even more sterically demanding NR_2 groups, e.g., N-*i*-Pr_2, which gives monomeric $Cr(N\text{-}i\text{-}Pr_2)_3$,[13] have thus far not led to any characterizable compounds by crystallization or sublimation techniques.

Physical Properties. $Mo_2(NR_2)_6$, where $NR_2 = NMe_2$, NMeEt, and NEt_2, are moisture and oxygen sensitive, yellow, crystalline, diamagnetic compounds and are appreciably soluble in alkane solvents. A cryoscopic molecular weight determination in benzene indicated the dinuclear nature of the dimethylamide, i.e., $Mo_2(NMe_2)_6$. Their mass spectra show strong parent ions, $Mo_2(NR_2)_6{}^+$, together with many other dimolybdenum fragments such as $Mo_2(NR_2)_5{}^+$ and $Mo_2(NR_2)_4{}^+$. A number of doubly charged Mo_2-containing ions were also observed. The presence of dimolybdenum ions produces a very characteristic isotopic distribution pattern. The observed vs. calculated pattern for $Mo_2(NMe_2)_6{}^+$ is shown in Figure 1. A characteristic feature of the mass spectra of these compounds is the absence of ions containing only one molybdenum atom.

The dinuclear, diamagnetic nature of these compounds together with the abundance of Mo_2-containing ions in their mass spectra provided evidence for the existence of strong Mo–Mo bonding Further evidence came from ^1H NMR studies.

^{1}H NMR Spectra. Solutions of $Mo_2(NMe_2)_6$ in toluene-d_8 show a single resonance, $\nu_{1/2} = 3.0$ Hz, at 3.28 ppm relative to HMDS (hexamethyldisiloxane) at 30° and above. This is comparable to other transition metal dimethylamides, e.g., compare $Mo(NMe_2)_4$, singlet δ 3.25 ppm, and $W(NMe_2)_6$, singlet, δ 3.33 ppm.

However, on cooling a sample of $Mo_2(NMe_2)_6$ the singlet at 3.28 ppm initially broadens until at −30° it is lost into the baseline. On further cooling two new resonances appear at δ 4.13 and 2.41 ppm. These are in the integral ratio 1:1 and sharpen on cooling to give $\nu_{1/2} = 4$ Hz at −71°. Further cooling of the sample to −90° produces no significant change except that the line width increases at low temperatures. These observations are independent of $Mo_2(NMe_2)_6$ concentration and independent of added Me_2NH.

The low-temperature limiting spectrum is clearly inconsistent with a dimeric bridged structure $(Me_2N)_2Mo(\mu\text{-}NMe_2)_2Mo(NMe_2)_2$ akin to that observed[14] for $Al_2(NMe_2)_6$ and suggested for $Ti_2(NMe_2)_6$. Furthermore, the marked shielding and deshielding experienced by the two types of methyl groups warrants a specific explanation.

It was these considerations which initially led us to suggest a dinuclear structure for $Mo_2(NMe_2)_6$ involving a Mo–Mo triple bond and six terminal NMe_2 ligands, with the planar Mo–NC_2 units in a propeller-like arrangement so as to produce six proximal and six distal methyl groups. The crystallographic characterization of this molecule (discussed later) clearly shows that in the crystalline state the methyl groups are directed over (proximal) and away from (distal) the Mo–Mo bond. The low-temperature limiting spectrum can thus readily be reconciled with the freezing out of a structure akin to that found in the crystal.

The large chemical shift difference betwen the proximal and distal methyl groups is not entirely surprising since a multiple metal–metal bond might be expected to have considerable magnetic anisotropy. A much smaller effect of this kind was reported earlier[15] for some compounds containing quadruple bonds. It will be shown later that experimental data for $Mo_2(NMeEt)_6$ indicate that the proximal resonance occurs downfield (δ 4.13) and the distal one upfield (δ 2.41). This assignment is reasonable from a theoretical point of view as well.

The magnetic susceptibility of the molecule should have a principal axis of symmetry along the M–M line. Both diamagnetic and (temperature-independent) paramagnetic moments could be introduced by the applied magnetic field. In view of the closed shell electronic structure of the molecule,

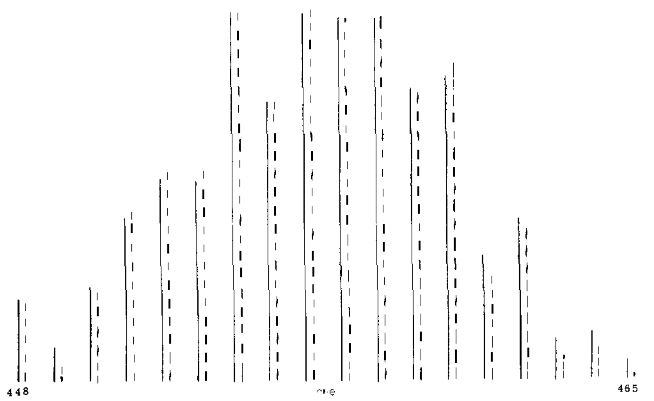

Figure 1. Observed (—) vs. calculated (- - -) m/e for $Mo_2(NMe_2)_6^+$.

with all metal-atom electrons in bonding orbitals, it seems unlikely that any electronic excited state suitable for producing a Van Vleck second-order paramagnetic moment under the action of the magnetic field could be of sufficiently low energy to do so to a significant extent. Thus, we expect the dominant magnetic field induced in the molecule to be in opposition to the applied field and symmetric about the molecular threefold axis. This will lower the effective field in the region of distal methyl groups and increase it in the region of proximal methyl groups, with the result that the signals for distal and proximal protons will lie, respectively, upfield and downfield from the nearly identical positions they would otherwise have had.

Regardless of whether the above assignment is correct, the temperature dependence of the proton NMR spectrum of $Mo_2(NMe_2)_6$ can be used to estimate the free energy of activation for proximal-distal exchange. Using the Gutowsky-Holm equation,[16] which is rigorously appropriate to this case, we estimate $\Delta G^{\ddagger} = 11.5 \pm 0.2$ kcal mol^{-1} at the coalescence temperature of -30 ± 2 °C.

Mechanisms which interchange proximal and distal methyl groups could involve (i) a fluxional process in which NMe_2 groups are transferred from one molybdenum atom to the other, as in the now well-recognized phenomenon of CO ligand scrambling in polynuclear metal carbonyl complexes,[17] (ii) a dissociative process, i.e.,

$$Mo_2(NMe_2)_6 \rightleftharpoons Mo_2(NMe_2)_5^+ + {}^-NMe_2$$

and (iii) processes involving "rotation" about molybdenum-nitrogen bonds. For the latter, many "flip" rearrangements[18] are possible and we note the stereochemical correspondence of $Mo_2(NMe_2)_6$ to hexaphenyldisilane.

We cannot distinguish between these mechanisms since they are permutationally indistinguishable. We have attempted to synthesize compounds of the type $Mo_2(NMe_2)_5L$, where L = NPh_2 and I (see Experimental Section), since these could allow further insight into the mechanism of proximal and distal interchange. Our synthetic attempts were unsuccessful. However, $W_2(NEt_2)_4Cl_2$ has been isolated and characterized[9] and for this compound all available evidence points to a mechanism involving a rotation about the metal-nitrogen bonds.

The variable temperature ^{1}H NMR spectra of $Mo_2(NEt_2)_6$ parallel those observed for $Mo_2(NMe_2)_6$. At low temperatures proximal and distal ethyl groups are frozen out (proximal $\delta(CH_2)$ 4.76, $\delta(CH_3)$ 1.16 ppm, $^3J_{HH} = 7$ Hz; distal: $\delta(CH_2)$ 2.34, $\delta(CH_3)$ 0.82 ppm rel HMDS) and at high temperatures rapid averaging occurs on the NMR time scale ($\delta(CH_2)$ 3.63, $\delta(CH_3)$ 1.05 ppm (rel HMDS), $^3J_{HH} = 7$ Hz). We estimate the energy of activation for proximal-distal ethyl exchange to be 13.6 ± 0.5 kcal mol^{-1}. Thus the free energy of activation for proximal and distal alkyl exchange in $Mo_2(NR_2)_6$ is greater for R = Et than for R = Me, a fact which probably reflects the different steric demand of these groups.

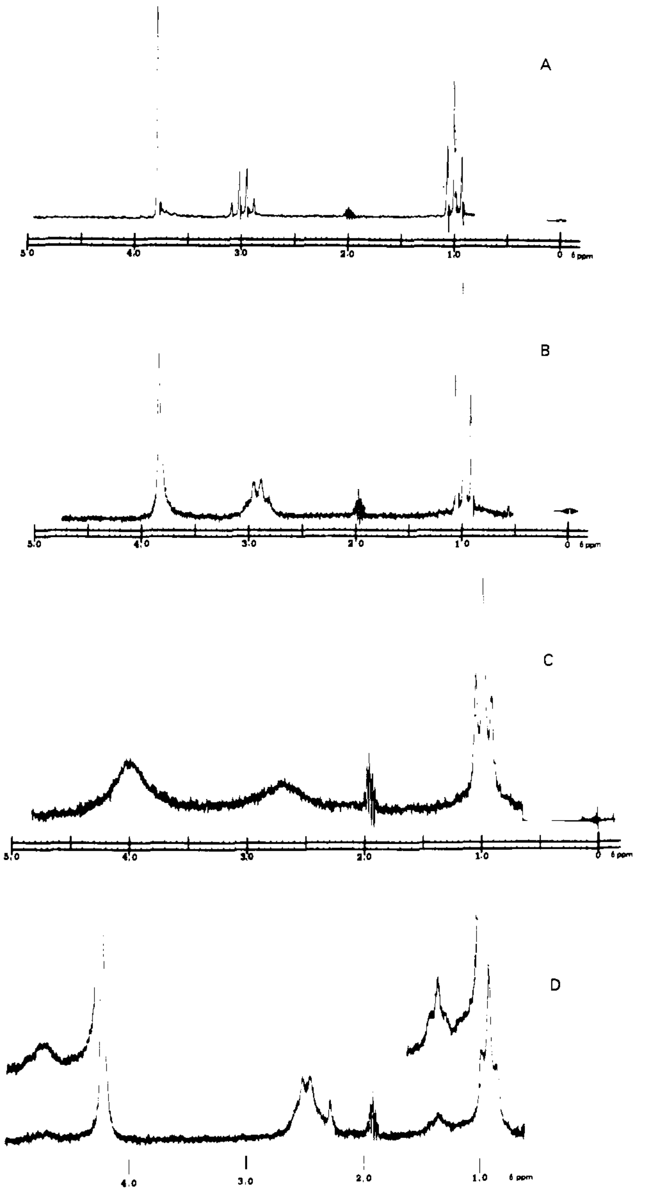

Figure 2. Variable temperature ^{1}H NMR spectra of $Mo_2(NMeEt)_6$ obtained in toluene-d_8 at 100 MHz: A at 81°; B at 40°; C at 0°; and D at −60°. δ in parts per million relative to HMDS.

The variable temperature ^{1}H NMR spectra of $Mo_2(NMeEt)_6$ are particularly interesting and warrant further comment. Representative spectra obtained over the temperature range +81° to −60° are shown in Figure 2. At +60° and above in toluene-d_8 $Mo_2(NMeEt)_6$ shows a single sharp *N*-methyl resonance at 3.81 ppm and single ethyl pattern: $\delta(CH_2)$ 2.97 and $\delta(CH_3)$ 1.00 ppm (rel HMDS), $^3J_{HH} = 7$ Hz. Compared to other metal methylethylamides the NMe resonance is to lower field while the NCH_2 resonance is at higher field. This may be compared with $Mo(NMeEt)_4$ for which $\delta(NMe)$ 3.17, $\delta(CH_2)$ 3.41, $\delta(CH_2CH_3)$ 1.08 ppm rel HMDS. (No significant chemical shift change with temperature is observed for $Mo(NMeEt)_4$.) On cooling a solution of $Mo_2(NMeEt)_6$ in toluene-d_8 below 60° the NMe resonance initially shifts slightly to lower field, broadens significantly, and then sharpens. A similar process is observed for the ethyl resonances which shift to higher field. The low temperature limiting spectrum is attained at −60°: $\delta(NMe)$ 4.23, $\delta(CH_2)$ 2.48, and $\delta(CH_2CH_3)$ 0.92 ppm, $^3J_{HH} = 7$ Hz. However, careful examination of the low temperature limiting spectrum reveals, in addition to the above, a singlet $\delta(NMe)$ 2.28, quartet $\delta(CH_2)$ 4.71, and triplet $\delta(CH_2CH_3)$ 1.36 ppm. We estimate

Table I. Atomic Positional Parameters

	x	*y*	*z*
Mo(1)	−0.007 29 (9)	0.429 37 (8)	0.453 42 (6)
Mo(2)	0.458 79 (9)	0.051 17 (9)	0.442 01 (6)
N(11)	0.073 6 (9)	0.484 0 (8)	0.359 6 (6)
N(12)	0.075 6 (9)	0.309 0 (8)	0.527 4 (7)
N(13)	−0.180 2 (9)	0.405 2 (9)	0.416 1 (7)
N(21)	0.567 0 (10)	0.032 8 (9)	0.358 0 (6)
N(22)	0.458 3 (9)	0.204 2 (8)	0.491 7 (7)
N(23)	0.299 1 (9)	−0.015 6 (9)	0.403 1 (6)
1C(11)	0.128 (1)	0.589 (1)	0.342 (1)
2C(11)	0.082 (1)	0.405 (1)	0.288 (1)
1C(12)	0.134 (1)	0.300 (1)	0.622 (1)
2C(12)	0.082 (1)	0.199 (1)	0.484 (1)
1C(13)	−0.283 (1)	0.464 (1)	0.441 (1)
2C(13)	−0.218 (1)	0.308 (1)	0.356 (1)
1C(21)	0.533 (1)	0.090 (1)	0.273 (1)
2C(21)	0.676 (1)	−0.034 (1)	0.362 (1)
1C(22)	0.500 (1)	0.250 (1)	0.579 (1)
2C(22)	0.403 (1)	0.290 (1)	0.430 (1)
1C(23)	0.219 (1)	0.038 (1)	0.324 (1)
2C(23)	0.235 (1)	−0.107 (1)	0.433 (1)

the concentration of the low field NMe resonance (δ 4.23 ppm) relative to the high field NMe (δ 2.28 ppm) resonance to be ca. 9:1. These observations clearly indicate that there are two (or more) isomers of $Mo_2(NMeEt)_6$ arising from the arrangements of proximal and distal methyl and ethyl groups and differing very little in free energy.

The structure of $Mo_2(NMe_2)_6$ reveals a marked difference between proximal Mo-N-C (132°) and distal Mo-N-C (116°) angles, which most likely reflects the great internal steric crowding of the molecule. Thus for $Mo_2(NMeEt)_6$ we would expect a ground state geometry with more proximal methyl groups than ethyl groups. This expectation is borne out in the low temperature limiting spectrum of $Mo_2(NMeEt)_6$.

At higher temperatures proximal-distal alkyl exchange rapidly interconverts these isomers and thus leads to the high temperature limiting spectrum shown in Figure 2.

Solid State Structure of $Mo_2(NMe_2)_6$. The atomic positional parameters are listed in Table I and the anisotropic temperature factors are given in Table II. The molecular dimensions are listed in Table III. Figure 3 shows the molecule viewed nearly along the Mo-Mo axis, so as to emphasize certain features of the molecular symmetry. Figure 3 also defines the atom numbering scheme. Since the molecules reside on crystallographic inversion centers the two ends are related and when numbers are required for atoms not explicitly numbered in the drawing (as in Table III), they are obtained by assigning them primed numbers corresponding to those of the atoms to which they are related by the inversion operation. For the second, crystallographically distinct molecule, an analogous numbering scheme is followed except that the metal atoms are

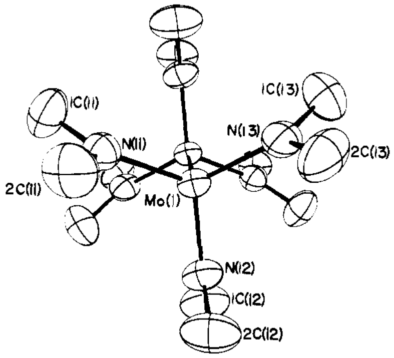

Figure 3. ORTEP view of $Mo_2(NMe_2)_6$ viewed nearly along the Mo-Mo axis.

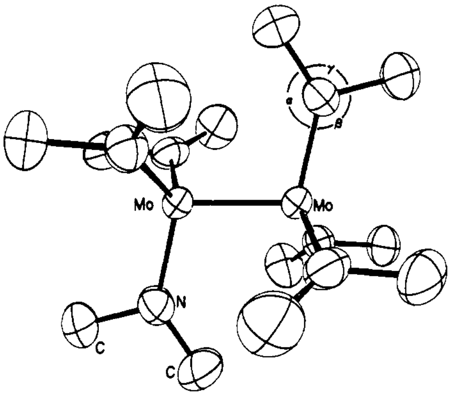

Figure 4. ORTEP view of $Mo_2(NMe_2)_6$ viewed nearly perpendicular to the Mo-Mo axis.

Table II. Anisotropic Temperature Factors[a] (×10^4)

	β_{11}	β_{22}	β_{33}	β_{12}	β_{13}	β_{23}
Mo(1)	75.6 (10)	53.2 (8)	27.0 (5)	3.0 (7)	7.1 (5)	−2.0 (5)
Mo(2)	73.9 (10)	67.2 (9)	25.5 (5)	8.2 (7)	0.8 (5)	1.7 (5)
N(11)	83 (10)	76 (9)	45 (6)	6 (8)	17 (6)	−3 (6)
N(12)	123 (12)	60 (9)	48 (6)	14 (8)	17 (7)	1 (6)
N(13)	90 (10)	83 (9)	44 (6)	−8 (8)	−5 (6)	5 (6)
N(21)	113 (12)	100 (10)	30 (5)	11 (9)	18 (6)	12 (6)
N(22)	113 (12)	72 (9)	43 (6)	−7 (8)	14 (6)	−16 (6)
N(23)	80 (10)	105 (10)	38 (5)	6 (8)	0 (6)	1 (6)
1C(11)	171 (20)	91 (14)	78 (10)	−19 (13)	58 (12)	8 (9)
2C(11)	144 (18)	104 (14)	48 (8)	19 (12)	29 (9)	−18 (8)
1C(12)	184 (21)	110 (15)	48 (8)	23 (14)	−11 (10)	4 (9)
2C(12)	173 (20)	84 (13)	60 (9)	41 (13)	16 (10)	−16 (8)
1C(13)	91 (15)	164 (20)	81 (11)	8 (14)	21 (10)	−11 (11)
2C(13)	149 (17)	87 (13)	57 (9)	−46 (12)	−10 (9)	6 (8)
1C(21)	153 (18)	119 (15)	27 (6)	12 (12)	15 (8)	15 (8)
2C(21)	106 (15)	140 (17)	82 (10)	48 (13)	40 (10)	25 (10)
1C(22)	167 (19)	110 (15)	44 (8)	0 (13)	19 (10)	−24 (8)
2C(22)	132 (16)	67 (12)	80 (10)	8 (11)	−1 (10)	28 (9)
1C(23)	129 (16)	107 (14)	40 (7)	31 (12)	−8 (8)	1 (8)
2C(23)	130 (17)	135 (17)	69 (10)	−24 (14)	10 (10)	22 (10)

[a] These are of the form exp $[-(\beta_{11}h^2 + \beta_{22}k^2 + \beta_{33}l^2 + 2\beta_{12}hk + 2\beta_{13}hl + 2\beta_{23}kl)]$.

Table III. Bond Distances (Å) and Angles (deg)

	Molecule I	Molecule II	Average[a]
Mo(*n*)-Mo(*n*)′	2.211 (2)	2.217 (2)	2.214 ± 0.003
Mo-N(*n*1)	1.98 (1)	1.98 (1)	
-N(*n*2)	1.97 (1)	2.00 (1)	
-N(*n*3)	1.97 (1)	1.98 (1)	1.98 ± 0.007
N(*n*1)-1C(*n*1)	1.45 (2)	1.46 (2)	
-2C(*n*1)	1.48 (2)	1.48 (2)	
N(*n*2)-1C(*n*2)	1.48 (2)	1.44 (2)	
-2C(*n*2)	1.50 (2)	1.46 (2)	
N(*n*3)-1C(*n*3)	1.49 (2)	1.51 (1)	
-2C(*n*3)	1.49 (2)	1.45 (2)	1.47 ± 0.02
Mo(*n*)-Mo(*n*)′-N(*n*1)	103.5 (3)	104.1 (3)	
-N(*n*2)	103.2 (3)	103.8 (3)	
-N(*n*3)	104.0 (3)	103.5 (3)	103.7 ± 0.3
N(*n*1)-Mo(*n*)-N(*n*2)	115.2 (4)	113.9 (4)	
-N(*n*3)	115.4 (4)	114.9 (4)	
N(*n*2)- -N(*n*3)	113.5 (4)	114.6 (4)	114.6 ± 0.6
Mo(*n*)-N(*n*1)-1C(*n*1)	134.9 (9)	132.4 (9)	
-N(*n*2)-1C(*n*2)	133.7 (9)	133.2 (9)	(α angles)
-N(*n*3)-1C(*n*3)	131.2 (9)	135.1 (9)	133.4 ± 1.2
Mo(*n*)-N(*n*1)-2C(*n*1)	116.2 (8)	116.4 (9)	
-N(*n*2)-2C(*n*2)	117.1 (9)	115.9 (8)	(β angles)
-N(*n*3)-2C(*n*3)	116.2 (9)	116.0 (9)	116.3 ± 0.3
1C(*n*1)-N(*n*1)-2C(*n*1)	108.9 (11)	111.2 (11)	
1C(*n*2)-N(*n*2)-2C(*n*2)	109.1 (11)	110.9 (11)	(γ angles)
1C(*n*3)-N(*n*3)-2C(*n*3)	112.5 (11)	108.8 (11)	110.2 ± 1.3

[a] For all dimensions, in both molecules, which would be equivalent under the symmetry operations of the group S_6.

Table IV. Unweighted Least-Squares Planes

	Equations of Planes[a]				
Plane no.	Atoms in plane	*A*	*B*	*C*	*D*
1	Mo(1)′-Mo(1)-N(11)	8.91	−4.33	5.17	0.420
2	Mo(1)′-Mo(1)-N(12)	−10.6	−3.27	6.62	1.68
3	Mo(1)′-Mo(1)-N(13)	−1.47	−7.58	11.7	2.07
4	Mo(2)′-Mo(2)-N(21)	5.23	9.50	4.66	4.95
5	Mo(2)′-Mo(2)-N(22)	−11.1	−2.01	6.08	−2.49
6	Mo(2)′-Mo(2)-N(23)	−5.69	7.43	10.6	2.45
7	1C(11)-N(11)-2C(11)	9.06	−3.79	5.25	0.723
8	1C(12)-N(12)-2C(12)	−10.8	−3.11	6.29	1.54
9	1C(13)-N(13)-2C(13)	−1.13	−7.08	12.2	2.40
10	1C(21)-N(21)-2C(21)	5.64	9.43	4.08	4.97
11	1C(22)-N(22)-2C(22)	−10.9	−2.38	6.46	−2.31
12	1C(23)-N(23)-2C(23)	−5.66	7.41	10.6	2.48

Dihedral Angles between Planes, deg		
Plane no.	Plane no.	Angle
1	7	2.7
2	8	1.7
3	9	3.6
4	10	2.7
5	11	2.4
6	12	0.3

[a] These equations are of the form $AX + BY + CZ = D$.

Table V

$Mo_2(NMe_2)_6$		$Mo_2(N(CD_3)_2)_6$	
Ir[a] (cm^{-1})	Raman[b] (cm^{-1})	Ir[a] (cm^{-1})	Raman[b] (cm^{-1})
1169 w	—	1064 m	—
—	1155 w	—	1033 w
1148 s	—	1028 m	—
1119 m	—	950 w	—
—	1083 w	—	—
1047 s	—	898 s	—
—	969 vs, p	—	833 s, p
959 s	—	825 s	—
944 vs	943 m	815 s	818 sh
552 vs	—	495 vs	499 sh
—	550 s, p	—	485 vs, p
—	409 w	—	401 w
—	361 m	—	326 m
356 s	—	320 s	—
—	319 s, p	—	284 s, p
312 m	—	275 w	—
—	228 s, p	—	206 s, p
—	—	—	136 w
—	105 w	—	—

[a] Nujol mull with CsI plates; ±2 cm^{-1}. [b] Solid samples in capillary tubes, ±2 cm^{-1}.

denoted Mo(2) and Mo(2)′ and for the C and N atoms the numbers in parentheses have 2 rather than 1 for their first digit.

Figure 4 shows another view of the molecule in which several of the types of angles listed in Table III are defined.

The views shown in Figures 3 and 4, especially that in Figure 3, stress that the molecules have approximate symmetry which is far higher than that ($\bar{1}$) crystallographically required, namely, at least $S_6(\bar{3})$ or even $D_{3d}(\bar{3}m)$. The configuration around each nitrogen atom is essentially planar. That is, each set of atoms, Mo-N-C_2, is almost exactly coplanar. This is evidenced by the fact that in each of the six crystallographically independent groups the sum of the three bond angles about the nitrogen atom is 359.9 or 360.0°. In addition, the dihedral angles between the NC_2 planes and the Mo-Mo-N planes (Table IV) are all nearly the same, varying only from 0.3 to 3.6°. If these angles were exactly equal the symmetry would be $S_6(\bar{3})$. If these angles were all equal to zero, the symmetry would be $D_{3d}(\bar{3}m)$.

Vibrational Spectra. Infrared and Raman data for $Mo_2(NMe_2)_6$ are given in Table V and the Raman spectra for this compound and its perdeutero analogue are shown in Figure 5. The strong, polarized Raman bands at 550, 319, and 228 cm^{-1} are of particular interest since stretching of the Mo-Mo bond should contribute heavily to one or more a_{1g} normal modes and these should give rise to strong, polarized Raman bands. In an earlier, tentative assignment, it was suggested[10] that the band at 228 cm^{-1} might be considered as, approximately, ν_{str}(Mo-Mo), and that the band at 319 cm^{-1} might be assigned to $\delta(NC_2)$, the latter assignment being derived from comparison with spectra of other dimethylamido compounds. We now recognize that these assignments are naive, and that the vibrational spectra of this and similar molecules are probably not subject to any such simple, "first order" assignments.

We have used a modified form of Badger's rule given by Herschbach and Laurie.[19] Using the values[20] $d = 0.88$ and $a = 2.73$ in eq 7 of ref 19, together with a value of 2.22 Å for r_e(Mo-Mo), we estimated a force constant for the Mo-Mo triple bond of 2.57 mdyn/Å. If there were a pure Mo-Mo stretching mode, which could be treated in the harmonic oscillator approximation, its frequency would then be calculated as about 333 cm^{-1}. This result would suggest a reversal of the earlier assignment mentioned above. The "Mo-Mo stretching" frequencies in $Mo_2(NMeEt)_6$ and $Mo_2(NMe_2)_6$ would then, presumably, be assigned to bands at 319 and 288 cm^{-1}, respectively. In all cases, the band around 500 cm^{-1} would be assigned to Mo-N stretching.

However, we now have evidence to show that these assignments are far too simplistic. As can be seen in Figure 5 and Table V, when the methyl groups are deuterated there are substantial shifts in all three of the strong, polarized Raman bands under discussion. This means that all of them must be

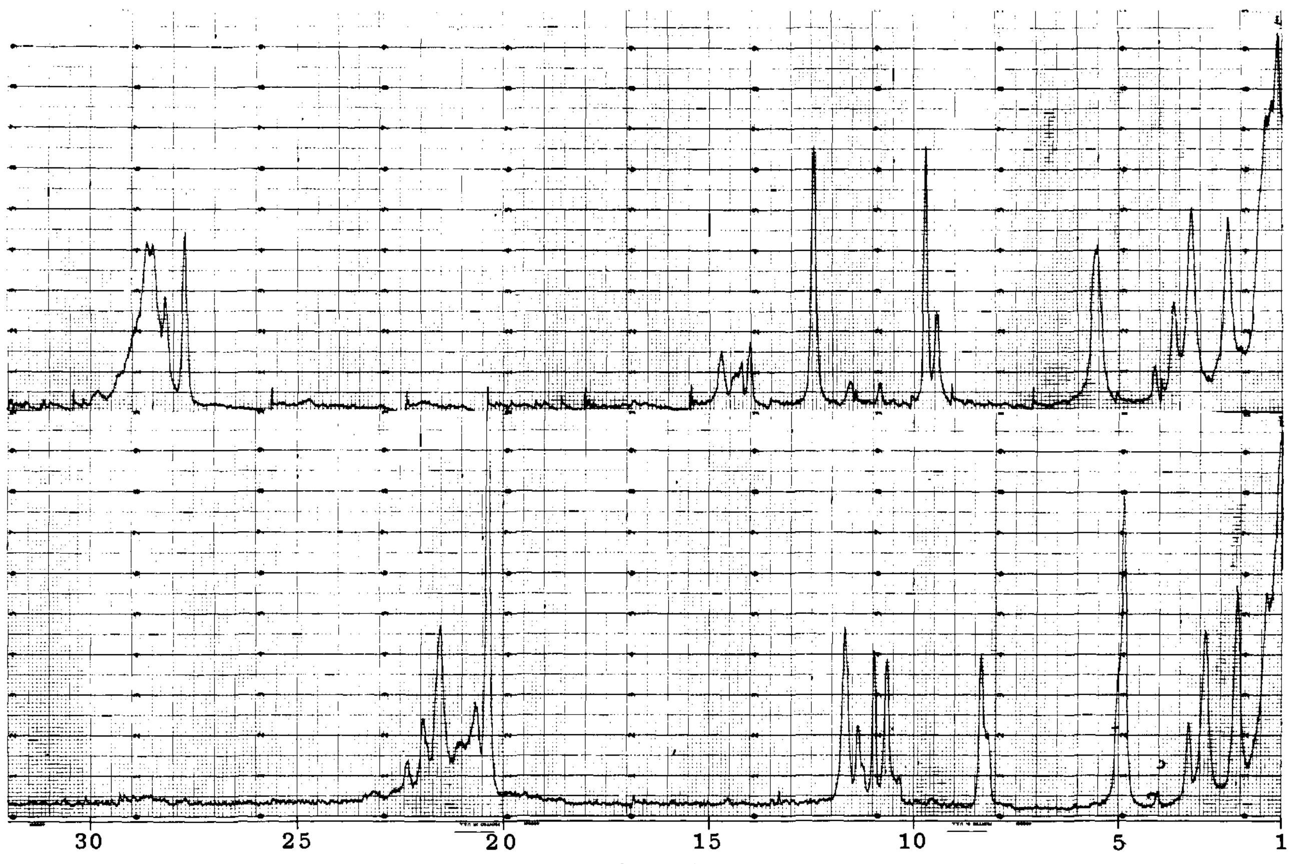

Figure 5. Raman spectrum of a polycrystalline sample of $Mo_2(N(CH_3)_2)_6$ (top) and $Mo_2(N(CD_3)_2)_6$ (bottom), in the range 3400–100 cm^{-1}.

due to normal modes in which there is considerable involvement of the hydrogen atoms. The band at 319 cm^{-1}, which shifts to 284 cm^{-1} cannot be considered as "the Mo–Mo stretching mode" to any useful approximation. As will be seen in the following paper[8] $W_2(NMe_2)_6$ has strong, polarized Raman bands at very similar frequencies, 550, 322, and 213 cm^{-1}. This vitiates any assignment in which a reasonably pure metal–metal stretching mode could be found for each molecule, with their frequencies being in the inverse ratio of the square roots of their masses.

It is particularly interesting that $Mo_2(NR_2)_6$ do not show strong Raman bands which can be simply assigned to ν_{str}(Mo–Mo) since inorganic chemists have become accustomed to thinking that compounds with metal–metal bonds, especially those with M–M multiple bonds, characteristically show easily recognizable Raman active bands assignable to M–M stretching modes.[21]

Bonding in $Mo_2(NMe_2)_6$. The bonding in $Mo_2(NMe_2)_6$ can be qualitatively described as follows: Each molybdenum atom forms four σ-bonds, three to nitrogen and one to the other molybdenum atom, utilizing approximately tetrahedral hybrid orbitals. These might be sp^3, sd^3, or any intermediate combination. Then, defining the Mo–Mo axis as the z axis, two metal–metal π-bonds can be formed employing d_{xz}, d_{yz} and/or p_x, p_y orbitals on each atom. The Mo–Mo triple bond so formed parallels that in $Mo_2(CH_2SiMe_3)_6$ and readily accounts for the short Mo–Mo distance, 2.214 (2) Å, the ethane-like Mo_2N_6 moiety, and the diamagnetic nature of the compound. However, for $Mo_2(NMe_2)_6$ the nitrogen lone pairs may also enter into the bonding scheme. Indeed the planarity of the Mo–NC_2 units together with the somewhat short Mo–N distances, 1.98 (1) Å, suggest that N to Mo π-bonding should be considered. In an idealized D_{3d} ground state configuration in which the plane of each NC_2 unit contains the Mo–Mo axis, the two pairs of molybdenum d_{xy} and $d_{x^2-y^2}$ atomic orbitals may accommodate eight electrons from nitrogen lone pairs. This leads to 16 valence shell electrons per molybdenum atom and leaves two nitrogen π-electron pairs in essentially nonbonding orbitals of a_{2g} and a_{1u} symmetry. The observed configuration for the $Mo_2(NC_2)_6$ group deviates but little from the D_{3d} configuration which, for convenience, we have assumed. The foregoing discussion of bonding is very speculative. In order to reach a more definite understanding of the electronic structure, we have begun studies of valence-shell photoelectron spectra and Xα-SW molecular orbital calculations.

It is also interesting to consider the other configuration of D_{3d} symmetry, in which the NC_2 planes would be perpendicular to the Mo–Mo–N planes. For steric reasons alone this would be very unfavorable. It would allow effective interaction of the nitrogen lone pair electrons with the metal atom orbitals (p_z, d_{xz}, d_{yz}) but to the extent that these interactions became effective the metal–metal bond would have to be based more on overlap of $d_{x^2-y^2}$ and d_{xy} orbitals. Since these δ overlaps would be far weaker than dπ–dπ overlaps, this would probably be electronically unfavorable. The observed structure is thus the expected one on both steric and electronic grounds.

The Mo–Mo distance in $Mo_2(NMe_2)_6$, 2.214 (2) Å, is longer than those generally observed in compounds containing Mo–Mo quadruple bonds but falls within the range expected for compounds with Mo–Mo triple bonds. It would appear to be significantly longer than that in $Mo_2(CH_2SiMe_3)_6$, 2.167 Å, although the error in the Mo–Mo distance in $Mo_2(CH_2SiMe_3)_6$ was not reported. Aside from the different steric requirements of NMe_2 and CH_2SiMe_3 ligands which could account for differences in the Mo–Mo distance, different electronic factors associated with these ligands should also be considered. In $Mo_2(NMe_2)_6$ ligand π-electrons are donated to metal orbitals which are δ and δ^* orbitals with respect to metal–metal bonding. This factor could lead to a lengthening of the Mo–Mo triple bond relative to that in $Mo_2(CH_2SiMe_3)_6$. The role of electronic factors in M–N triple bond distances is not well understood at this time. However, the long Mo–Mo distance, 2.448 (1) Å, in $Cp_2Mo_2(CO)_4$, which contains a linear CpMo–MoCp moiety and by simple valence electron counting might be supposed to have a Mo–Mo triple bond, further indicates the influence of electronic factors on M–M bond distance. This point is discussed further in a following paper on $W_2(NMe_2)_6$.

Experimental Section

Materials. $MoCl_5$ was purchased (or received as a gift) from Climax Molybdenum Company. $MoCl_3$ was prepared according to the method of Mallock.[22] $LiNMe_2$ was prepared by condensing an equimolar amount of dimethylamine (Matheson) into a cold (ca. −70°) ether/hexane solution of *n*-butyllithium (Alfa). LiNMeEt and $LiNEt_2$ were prepared similarly. HNMeEt was obtained from the Ames Laboratory, $HNEt_2$ from Matheson Coleman and Bell. $HN(CD_3)_2$ was purchased from Merck, Sharp and Dohme.

Physical and Analytical Measurements. Elemental analyses were performed by Alfred Bernhardt Mikroanalytisches Laboratorium, West Germany, using drybox sampling techniques. Molecular weight determinations were made under a purified nitrogen atmosphere in an all-glass cryoscopic apparatus incorporating a thermister bridge.

Electronic absorption spectra were measured with a Perkin-Elmer 202 spectrophotometer using quartz cells of 1-cm pathlength fitted with a Teflon–quartz seal.

Infrared spectra were obtained from Nujol mulls or from solutions in hexane between CsI plates/windows using a Beckman IR-12 spectrophotometer.

Raman spectra were obtained on a spectrophotometer equipped with a coherent Radiation Model CR5 Ar^+ laser, a Spex Model 1401 double monochromator, and a cooled ITT FW-130 Startracker photomultiplier tube using the 5145 Å exciting line. Spectra of solid samples were obtained from capillary tubes sealed under N_2; solution spectra were obtained in THF using a Spex rotating quartz cell adapted for air-sensitive work.

^1H NMR spectra were obtained from a Varian HA-100 spectrometer equipped with a variable temperature probe. Temperatures were calibrated with ethylene glycol (high temperature) and methanol (low temperature) before and after each set of spectra. Hexamethyldisiloxane (HMDS) was chosen as the internal reference.

Mass spectra were obtained on an AEI MS 9 by the method of direct insertion with probe temperatures 100–120°.

General Procedures. Due to the highly reactive nature of $LiNR_2$, $Mo_2(NR_2)_6$, and related compounds, all preparations and other operations were carried out under a dry and oxygen-free nitrogen atmosphere or in vacuo. Solvents were dried and freed from dissolved molecular oxygen by distillation from a solution of the solvent, benzophenone, phenyl ether, and sodium. When not needed for immediate use, solvents were stored over calcium hydride under nitrogen. Samples were stored and handled in a Vacuum Atmospheres Dri Lab System.

Preparation of Hexakis(dimethylamido)dimolybdenum(III). (a) From the Reaction of $MoCl_3$ with $LiNMe_2$. $MoCl_3$ (23.0 g, 114 mmol) was added in portions to an ice-cold magnetically stirred solution of $LiNMe_2$ (341 mmol) in hexane (150 ml), ether (100 ml), and THF (200 ml) over a period of 1 h. (*Caution:* an exothermic reaction occurs.) The reaction mixture was then allowed to warm to room temperature and stirred for a further 8 h. Solvent was then removed in vacuo, and the resulting brown solids were heated to 70° at 10^{-4} cmHg for 2 h. (This ensured removal of all THF and drove off the very volatile, purple $Mo(NMe_2)_4$.) Only a trace of $Mo(NMe_2)_4$ was liberated. Hexane (120 ml) and pentane (50 ml) were added to the dried solids to give a dark brown solution and finely divided gray solids. The solution was filtered using standard Schlenk tube techniques, and the solids were repeatedly washed with pentane/hexane, distilled under vacuum from the filtrate solution through the frit. (This procedure avoids the necessity of introducing additional solvent.) The filtrate was then evaporated to dryness in vacuo yielding a crude sample of $Mo_2(NMe_2)_6$. Pure yellow crystalline $Mo_2(NMe_2)_6$ (4.8 g) was obtained by sublimation from this crude material at 100–120°, 10^{-4} cmHg, over a period of 6 h. Anal. Calcd (found) for $Mo_2(NMe_2)_6$: C, 31.59 (31.29); H, 7.95 (7.71); N, 18.42 (18.17). Parent ion at *m/e* 456 in the mass spectrum corresponds to $Mo_2(NMe_2)_6{}^+$ (based on ^{96}Mo).

(b) From the Reaction of $MoCl_5$ with $LiNMe_2$. $MoCl_5$ (21.9 g, 80 mmol) was added in portions to an ice-cold magnetically stirred slurry of $LiNMe_2$ (400 mmol) in hexane (150 ml) and ether (200 ml) over a period of 1 h. An exothermic reaction occurred. The reaction mixture was then allowed to warm to room temperature and was stirred for a further 6 h at which time the solvent was stripped off. Hexane (150 ml) and pentane (50 ml) were added to the above and the dark brown solution so formed was separated from the solids (mostly LiCl) by standard Schlenk tube filtration techniques. The filtrate was evaporated to dryness to yield a sticky brown solid, which on heating, 40–70° at 10^{-4} cmHg, yielded the highly volatile purple $Mo(NMe_2)_4$. The latter was collected on the probe of a cold finger cooled with solid CO_2. $Mo(NMe_2)_4$ obtained in this manner was collected by washing the probe with pentane. The brown residues (crude $Mo_2(NMe_2)_6$) were then extracted with hexane (100 ml) and pentane (25 ml), filtered, and dried. Upon heating to 40–70° at 10^{-4} cmHg more $Mo(NMe_2)_4$ sublimed and was collected as above. This process was repeated a further two times until only a trace of $Mo(NMe_2)_4$ sublimed. The residue was then heated to 100–120° at 10^{-4} cmHg for 6 h during which time the yellow crystalline solid $Mo_2(NMe_2)_6$ sublimed (2.4 g).

$Mo_2(NMe_2)_6$ can be recrystallized from hexane or toluene solutions. Note that $Mo_2(NMe_2)_6$ is an exceedingly oxygen- and moisture-sensitive compound and reacts with many common organic solvents (e.g., CS_2, acetone, alcohols, $CHCl_3$, CCl_4). However, $Mo_2(NMe_2)_6$ is appreciably soluble in alkane solvents and appears indefinitely stable at room temperature providing it is kept under vacuum or stored under an inert atmosphere such as N_2.

Preparation of $Mo_2(N(CD_3)_2)_6$. As in procedure (a) above using $LiN(CD_3)_2$. Parent ion at *m/e* 492 in the mass spectrum corresponded to $Mo_2(N(CD_3)_2)_6$ (based on ^{96}Mo).

Preparation of Hexakis(diethylamido)dimolybdenum(III). $MoCl_3$ (17.7 g, 87 mmol) was added in portions to an ice-cooled magnetically stirred solution of $LiNEt_2$ (260 mmol) in hexane (100 ml), ether (150 ml), and THF (150 ml) over a period of 1 h. An exothermic reaction occurred. The reaction mixture was then allowed to warm to room temperature and stirred for a further 8 h at which time the solvent was stripped off. The solids thus formed were dried at 40°, 10^{-4} cmHg, for 2 h to ensure complete removal of THF and $HNEt_2$. Extraction with hexane (150 ml) and pentane (50 ml) in the manner previously described for the preparation of $Mo_2(NMe_2)_6$ yielded a brown sticky solid from which a purple liquid, $Mo(NEt_2)_4$, distilled at 100–120°, 10^{-4} cmHg. The latter was collected and the residue containing $Mo_2(NEt_2)_6$ was again extracted with hexane (50 ml) and pentane (25 ml). At 100–120°, 10^{-4} cmHg, some $Mo(NEt_2)_4$ again distilled. This was collected, and the brown residues were then heated to 140–170° at 10^{-4} cmHg for 6 h during which time a yellow crystalline solid, $Mo_2(NEt_2)_6$, sublimed. This solid was scraped loose from the sublimer, dissolved in hexane (20 ml), and crystallized by slowly cooling to −78°. This yielded $Mo_2(NEt_2)_6$ as a pale yellow crystalline compound (1.2 g). Anal. Calcd for $Mo_2(NEt_2)_6$; C, 46.14; H, 9.68; N, 13.46. Found: C, 45.88; H, 9.36; N, 13.21. Parent ion in the mass spectrum at *m/e* 624 corresponds to $Mo_2(NEt_2)_6{}^+$ (based on ^{96}Mo).

Preparation of Hexakis(ethylmethylamido)dimolybdenum(III). $MoCl_3$ (11.2 g, 55 mmol) was treated with LiNMeEt (165 mmol) in hexane (60 ml), ether (150 ml), and THF (150 ml) in a directly analogous procedure to that previously described for the preparation of $Mo_2(NEt_2)_6$. Extraction with hexane/pentane and subsequent sublimation, 50–80°, 10^{-4} cmHg, gave purple $Mo(NMeEt)_4$ which was collected on a probe cooled with liquid nitrogen. Extraction of the residue with hexane/pentane and sublimation at 100–130°, 10^{-4} cmHg, gave a yellow waxy solid. Crystallization from hexane gave $Mo_2(NMeEt)_6$ as a crystalline substance (1.0 g) Anal. Calcd for $Mo(NMeEt)_6$: C, 40.01; H, 8.95; N, 15.55. Found: C, 39.77; H, 8.76; N, 15.39. Parent ion at *m/e* 540 in the mass spectrum corresponds to $Mo_2(NMeEt)_6{}^+$ (based on ^{96}Mo).

Attempted Thermolysis of $Mo(NEt_2)_4$. $Mo(NEt_2)_4$ (1 g) was dissolved in hexane (10 ml), ether (10 ml), and THF (10 ml) to give a deep purple solution. The solution was then heated to reflux for 3 h. Upon removal of the solvent a purple viscous liquid remained. This was distilled at 80–100°, 10^{-4} cmHg, and was shown to be $Mo(NEt_2)_4$ by ^1H NMR spectroscopy. No significant decomposition was observed and no $Mo_2(NEt_2)_6$ was detected.

Reaction of $Mo(NEt_2)_4$ with $LiNEt_2$. $Mo(NEt_2)_4$ (1.0 g) was dissolved in hexane (15 ml) and a solution of $LiNEt_2$ (0.5 g) in THF (15 ml) was added. The solution was refluxed for 4 h at which time the solvent was stripped off to give a purple sticky solid. Upon heating this residue to 80–100°, 10^{-4} cmHg, $Mo(NEt_2)_4$ distilled off. This was characterized by ^1H NMR spectroscopy. At 140°, 10^{-4} cmHg, $LiNEt_2$ sublimed as a white crystalline solid. No $Mo_2(NEt_2)_6$ was detected.

Reaction of $Mo_2(NMe_2)_6$ with Ph_2NH. $Mo_2(NMe_2)_6$ (0.515 g, 1.13 mmol) was dissolved in benzene (10 ml) in a round-bottomed flask fitted with a condenser and containing a magnetic stirring bar. To this solution Ph_2NH (0.191 g, 1.13 mmol) dissolved in benzene (20 ml) was added with stirring. The solution was heated to reflux for 4 h at which time the solvent was stripped off. A sample of the solids remaining was examined by ^1H NMR spectroscopy which suggested that only pure $Mo_2(NMe_2)_6$ and Ph_2NH were present; i.e., no aminolysis had occurred. Heating this mixture to 40° at 10^{-3} cmHg caused Ph_2NH to sublime leaving behind pure $Mo_2(NMe_2)_6$.

Reaction of n-$Bu_4N^+I^-$ with $Mo_2(NMe_2)_6$. $Mo_2(NMe_2)_6$ (0.397 g, 0.87 mmol) and n-$Bu_4N^+I^-$ (0.321 g, 0.87 mmol) were placed in a 25-ml round-bottomed flask fitted with a condenser and a magnetic stirrer. Toluene (15 ml) was added and the solution was refluxed for 3 h. The solution was cooled slowly to −10° which resulted in the formation of white crystals. These were removed by filtration and identified as n-Bu_4NI. The filtrate was evaporated to dryness and examined by ^1H NMR spectroscopy which indicated the presence of $Mo_2(NMe_2)_6$ contaminated with n-Bu_4NI. Recrystallization from toluene gave pure $Mo_2(NMe_2)_6$.

Determination of Crystal Structure. A yellow crystal of approximate dimensions 0.3 × 0.2 × 0.2 mm was sealed in a capillary with epoxy glue. An alignment photograph was taken on a Syntex P1 four-circle automatic diffractometer, and 15 reflections from this photograph were used in the automatic centering procedure. The peak widths at half-height for several of these reflections were measured in ω-scans and found to be about 0.15°. Least-squares refinement of the 15 reflections gave an orientation matrix for calculation of setting angles and cell parameters. A monoclinic cell, later shown by systematic absences and successful refinement to belong to space group $P2_1/c$, was used. The cell dimensions are: $a = 11.461$ (3) Å, $b = 12.052$ (4) Å, $c = 15.409$ (3) Å, $\beta = 101.83$ (2)°, and $V = 2083.3$ (10) Å^3. For $Z = 4$, density (calcd) = 1.454 g cm^{-3}.

Data were collected at 23 ± 1° using the θ-2θ scan technique. Scan speeds varied from 4 to 24° min^{-1} depending upon the intensity of the reflection. Scans of each peak were made from 0.7° below $K\alpha_1$ to 0.8° above $K\alpha_2$. Three reflections were used as standards and their intensities were periodically monitored. All three decreased linearly during data collection with a total drop of ~30%, indicating crystal decomposition. All reflections remained intense enough to complete data collection on the same crystal.

Mo $K\alpha$ radiation, filtered by a graphite crystal monochromator, gave 3041 reflections in the 2θ range 0–45°. During data reduction, a linear correction for crystal decomposition was made, resulting in 1897 reflections with $F_o^2 > 3\sigma(F_o^2)$ which were used to solve and refine the structure.

The positions of two molybdenum atoms were taken from a three-dimensional Patterson map[23] and their positional and thermal parameters were refined in two cycles of full-matrix least-squares refinement. The resulting residuals were $R_1 = \Sigma||F_o| - |F_c||/\Sigma|F_o| = 0.264$ and $R_2 = (\Sigma w(|F_o| - |F_c|)^2/\Sigma wF_o^2)^{1/2} = 0.354$. A difference electron density map then revealed all non-hydrogen atoms. Three cycles of isotropic refinement followed by three cycles of anisotropic refinement resulted in residuals of 0.057 and 0.075. In a final difference electron density map peaks which might correspond to a few of the methyl hydrogen atoms were observed. However, since the majority could not be found and rotational disorder of the methyl groups is very likely, no hydrogen atoms were included in the refinement. The error in an observation of unit weight was 1.57 when a value of 0.07 was assigned to the parameter p used in the weighting function. Scattering factors from Cromer and Waber[24] including anomalous dispersion contributions[25] for molybdenum were used. No unusual trends were observed in the weighted residuals as a function of reflection number, $\lambda^{-1} \sin\theta$, $|F_o|$, or various classes of Miller indices. The observed and final calculated structure factor amplitudes, expressed as $10|F_o|$ and $10|F_c|$, are available.[26]

Acknowledgments. We thank Research Corporation, the donors of the Petroleum Research Fund, administered by the American Chemical Society, and the National Science Foundation (Grant GP-42691X) for support of this work at Princeton University and the National Science Foundation (GP33142X) at Texas A&M University. We also thank Climax Molybdenum Company for gifts of molybdenum halides.

Supplementary Material Available: A list of structure factor amplitudes (14 pages). Ordering information is given on any current masthead page.

References and Notes

(1) (a) Princeton University; (b) Texas A&M University.
(2) F. A. Cotton, *Chem. Soc. Rev.*, **4**, 27 (1975).
(3) F. Huq, W. Mowat, A. Shortland, A. C. Skapski, and G. Wilkinson, *Chem. Commun.*, 1079 (1971).
(4) M. H. Chisholm, W. W. Reichert, F. A. Cotton, B. A. Frenz, and L. Shive, *J. Chem. Soc., Chem. Commun.*, 480 (1974).
(5) R. J. Klingler, W. Butler, and M. D. Curtis, *J. Am. Chem. Soc.*, **97**, 3535 (1975).
(6) In this last paper no comment was made concerning this remarkable difference; in fact, the earlier examples of Mo–Mo triple bonds were not cited at all.
(7) F. A. Cotton, B. R. Stults, J. M. Troup, M. H. Chisholm, and M. Extine, *J. Am. Chem. Soc.*, **97**, 1242 (1975).
(8) M. H. Chisholm, F. A. Cotton, M. Extine, and B. R. Stults, *J. Am. Chem. Soc.*, **98**,4477 (1976).
(9) M. H. Chisholm, F. A. Cotton, M. Extine, M. Millar, and B. R. Stults, *J. Am. Chem. Soc.*, 98, 4486 (1976).
(10) M. H. Chisholm and W. Reichert, *J. Am. Chem. Soc.*, **96**, 1249 (1974).
(11) D. C. Bradley and M. H. Chisholm, *J. Chem. Soc. A*, 2741 (1971).
(12) J. S. Basi, D. C. Bradley, and M. H. Chisholm, *J. Chem. Soc. A*, 1433 (1971). The structure shown in eq 1 for $[Cr(NEt_2)_3]_2$ is inferred from indirect evidence and has not been verified crystallographically.
(13) D. C. Bradley, C. W. Newing, and M. B. Hursthouse, *Chem. Commun.*, 411 (1971).
(14) D. C. Bradley, *Adv. Inorg. Chem. Radiochem.*, **15**, 259 (1972), and references therein.
(15) J. San Filippo, Jr., *Inorg. Chem.*, **11**, 3140 (1972).
(16) J. A. Pople, W. G. Schneider, and H. J. Bernstein, "High Resolution NMR Spectroscopy", McGraw-Hill, New York, N.Y., 1959 p 223.
(17) R. D. Adams and F. A. Cotton, "Dynamic Nuclear Magnetic Resonance Spectroscopy", L. M. Jackman and F. A. Cotton Ed., Academic Press, New York, N.Y., 1975 p 489.
(18) K. Mislow, D. Gust, P. Finocchiaro, and R. J. Boetcher, *Top. Current Chem.*, **47**, 1 (1974); K. Mislow, *Acc. Chem. Res.*, **9**, 26 (1976).
(19) D. R. Herschbach and V. W. Laurie, *J. Chem. Phys.*, **35**, 458 (1961).
(20) A discussion of the evaluation of these parameters will be published elsewhere.
(21) B. I. Swanson, J. J. Rafalko, D. F. Shriver, J. San Filippo, and T. G. Spiro, *Inorg. Chem.*, **14**, 1737 (1975).
(22) A. Mallock, *Inorg. Nucl. Chem. Lett.*, **3**, 441 (1967).
(23) The following computer programs were used: DATARED by Frenz for data reduction; FAME, a program for calculating normalized structure factors by Dewar; JIMDAP, a version of Zalkin's Fourier program FORDAP, as modified by Ibers, NUCLS, a full-matrix least-squares program by Ibers and Doedens based on Busing and Levy's ORFLS program; RSCAN by Doedens for analysis of structure factors; ORTEP by Johnson for illustrations; ORFEE by Busing, Martin, and Levy as modified by Brown, Johnson, and Thiessen for distances and angles; LIST by Snyder for listing structure factors for publication.
(24) "International Tables for X-Ray Crystallography", Vol. IV, Kynoch Press, Birmingham, England.
(25) D. T. Cromer and D. Liberman, *J. Chem. Phys.*, **53**, 1891 (1970).
(26) See paragraph at end of paper concerning supplementary material.